

Released courtesy of Areva Resources Canada and UEX Corporation, the following document pertains to 3D inversion of a transient AMT (TAMT) data-set collected in the summer of 2005 approximately 600 km north-west of Saskatoon, SK (Figure's 1 and 2). Although the main feature(s) resolved by the data are related to conductive basement structure, sandstone resistivity is also mapped reasonably well, in good correlation with 3D inverted results of pole-pole DC resistivity data.



Figure 1: Regional Area Map

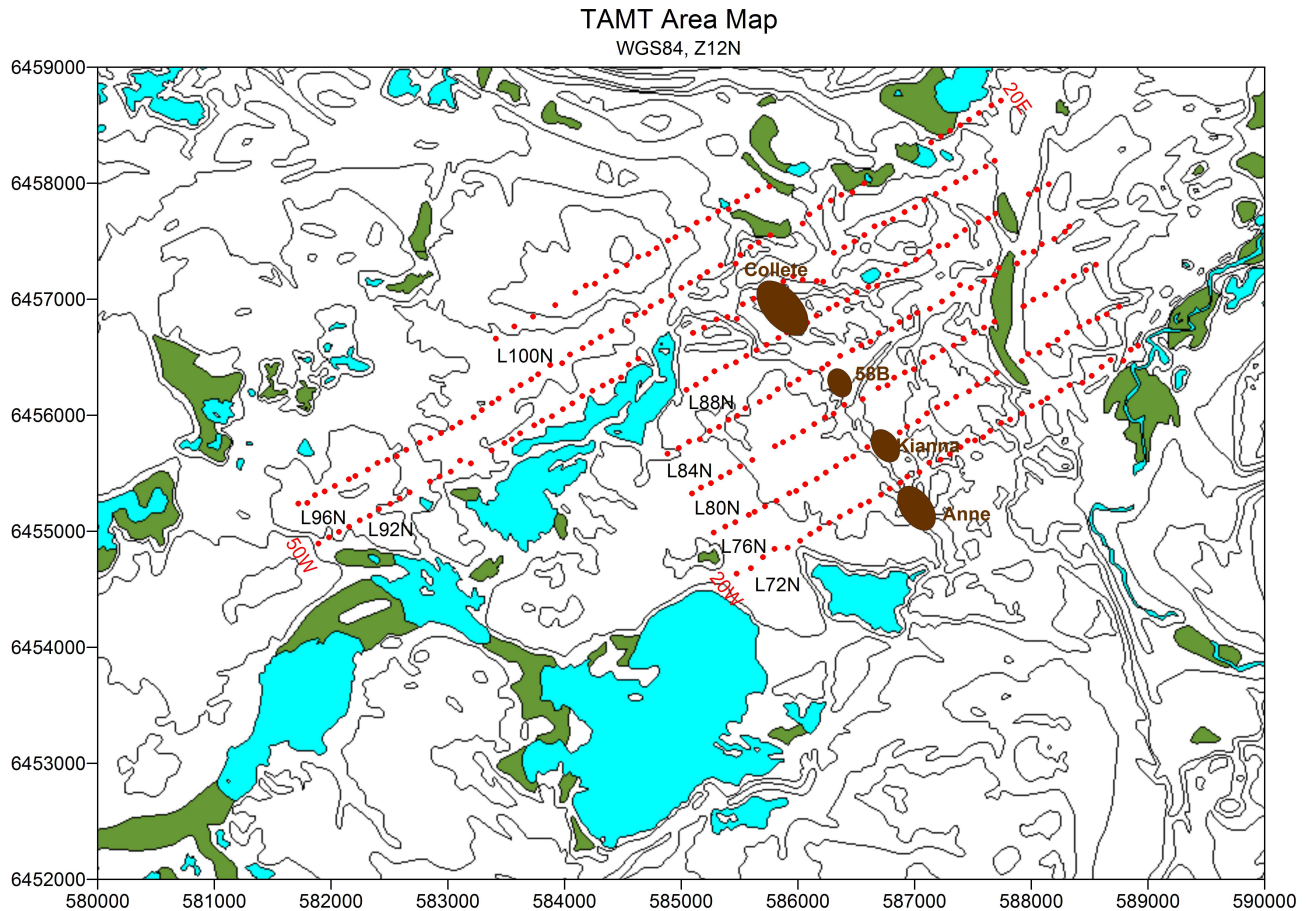


Figure 2: Local Area Map

Shown in Figure 3 is the plan view map of the 3D TAMT inverted results for the depth level 640 to 700 m¹. This can be compared to the 3D inversion of DC resistivity data at approximately 600 m depth shown in Figure 4 (Nimeck and Koch, 2007) with the TAMT station locations overlaid. Note that the plot scale and colour maps are slightly different in the two plots, the TAMT data is plotted on a log scale of 1 to 10,000 $\Omega - m$ while the DC resistivity data is plotted on a log scale of 50 to 10,000 $\Omega - m$.

A weakly conductive channel is seen in the TAMT inverted results over the Anne, Kianna and Colette deposits which correlates reasonably with that seen in the DC resistivity data. A resistive high encircled by conductive material is seen in the TAMT inverted results in the north-east corner of the inverted model, this again agrees with DC resistivity 3D inverted results. Evidence of sandstone alteration over the Klarke Lake conductor is also seen in the TAMT inverted results, although L92N and L96N were the only lines collected to 50W.

Interestingly, the results of tipper inversion alone (Figure 5) also show a weakly conductive channel above the Saskatoon Lake conductor (SLC) as well as a resistive high with encircling conductive material in the north-eastern corner of the model, but affects related to the Klarke Lake conductor are much more muted. This latter feature may be more formational in nature (flat lying conductive block), as opposed to structural (graphitic shear), due to its essentially absent tipper response but stronger impedance response².

In disagreement, the 3D TAMT inverted results show that the sandstone alteration over the SLC is “open” to the north-east (beyond L96N) and a resistivity low is seen in the TAMT inverted results on L100N, L96N and L92N in the 25W area. As well, the resistivity low in the north-east corner of the 3D TAMT model is much more pronounced as compared to the DC resistivity inverted results.

¹ Z_{xy}, Z_{yx}, T_x, T_y inversion but using the results of T_x, T_y 3D inversion alone as the initial and prior

²Compare also Figure 19, tipper only inversion on L96N to Figure 17 which includes the impedance

A vertical slice down L80N out of the 3D inverted cubes for both the DC resistivity and TAMT data-sets is shown in Figure's 6 and 7 respectively. Both results indicate a conductive halo in the sandstone above the SLC but the TAMT inverted results are not as smoothly varying and the conductive halo not as wide. Within the basement, the TAMT inverted results place conductive material around the top and western edges of the rather large (spatially), very smooth DC resistivity low feature.

The 3D inversion cube for the TAMT analysis is shown in Figure 8 with 3D volumetric plots showing material $\leq 30 \Omega\text{-m}$ in Figure 9 and $\leq 100 \Omega\text{-m}$ in Figure 10. Shallow conductive material, possibly related to Wolverine Point, is evident in Figure 10 on north-eastern portions of the survey grid, although a weak conductor may also be present at 6E on some lines (see below).

Vertical slices out of the 3D TAMT inversion cube, down the survey lines, is shown in Figure's 11 to 18. Conductive material above the SLC gets progressively displaced to the west, seen especially well between L72N and L80N. The progressive displacement appears to cease between L80N and L92N but begins on L96N again, with conductive material above the SLC now displaced to the west, being seen to "curl" at/near the unconformity. The movement of conductive material above the SLC may reflect cross cutting fault structure that is known to be present in the area.

Conductive material at the north-east end of lines is properly handled in the 3D inversion contained herein, this was problematic with previous 2D analysis. Furthermore, beginning on L80N, a small and relatively weak conductive trend is seen at approximately 700 m depth at 6E. However, this feature becomes more conductive (and deeper) on L92N, L96N (Figure's 16 and 17). More stations to the east would be required on L100N to ascertain it's character there.

The 3D TAMT model comprised thirty-three 200 m wide cells in the N-S direction by ninety-nine 100 m wide cells E-W and 36 cells vertically for 117,612 model parameters. The data at all 343 stations was simultaneously inverted at 15 frequencies for as many as 41,160 data parameters (Z_{xy} , Z_{yx} , T_x , T_y). This large inversion consumed slightly more than 53 GBytes of RAM and required 2.5 days to complete 6 iterations on our new Intel based cluster consisting of a dual processor, penta-core Xeon server with 96 GBytes of RAM with 6 quad core, core-i7 "slaves" for 36 cores total.

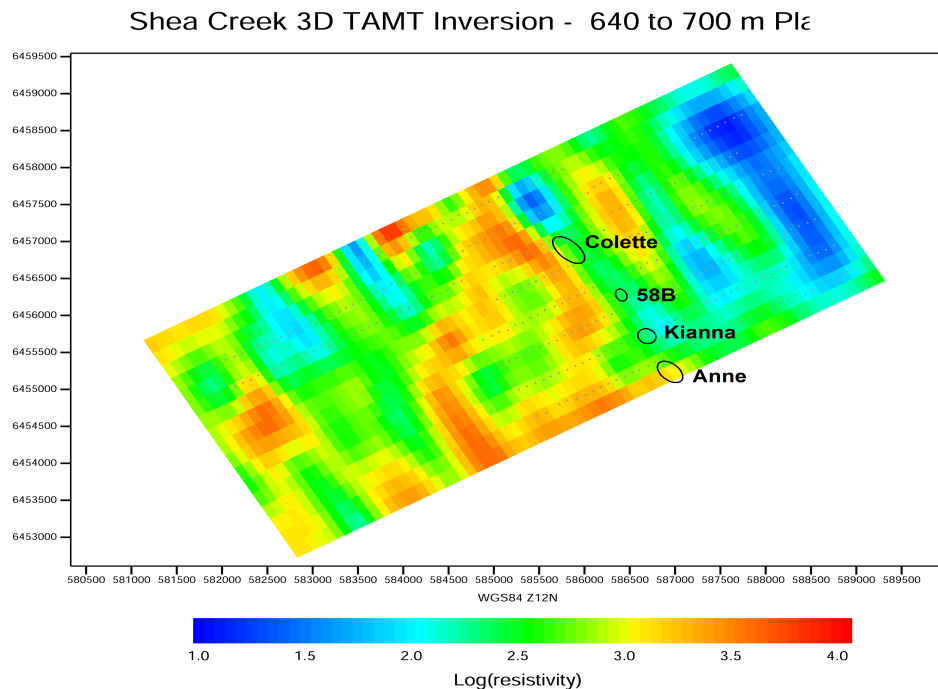


Figure 3: Horizontal slice out of joint impedance-tipper 3D inverted model

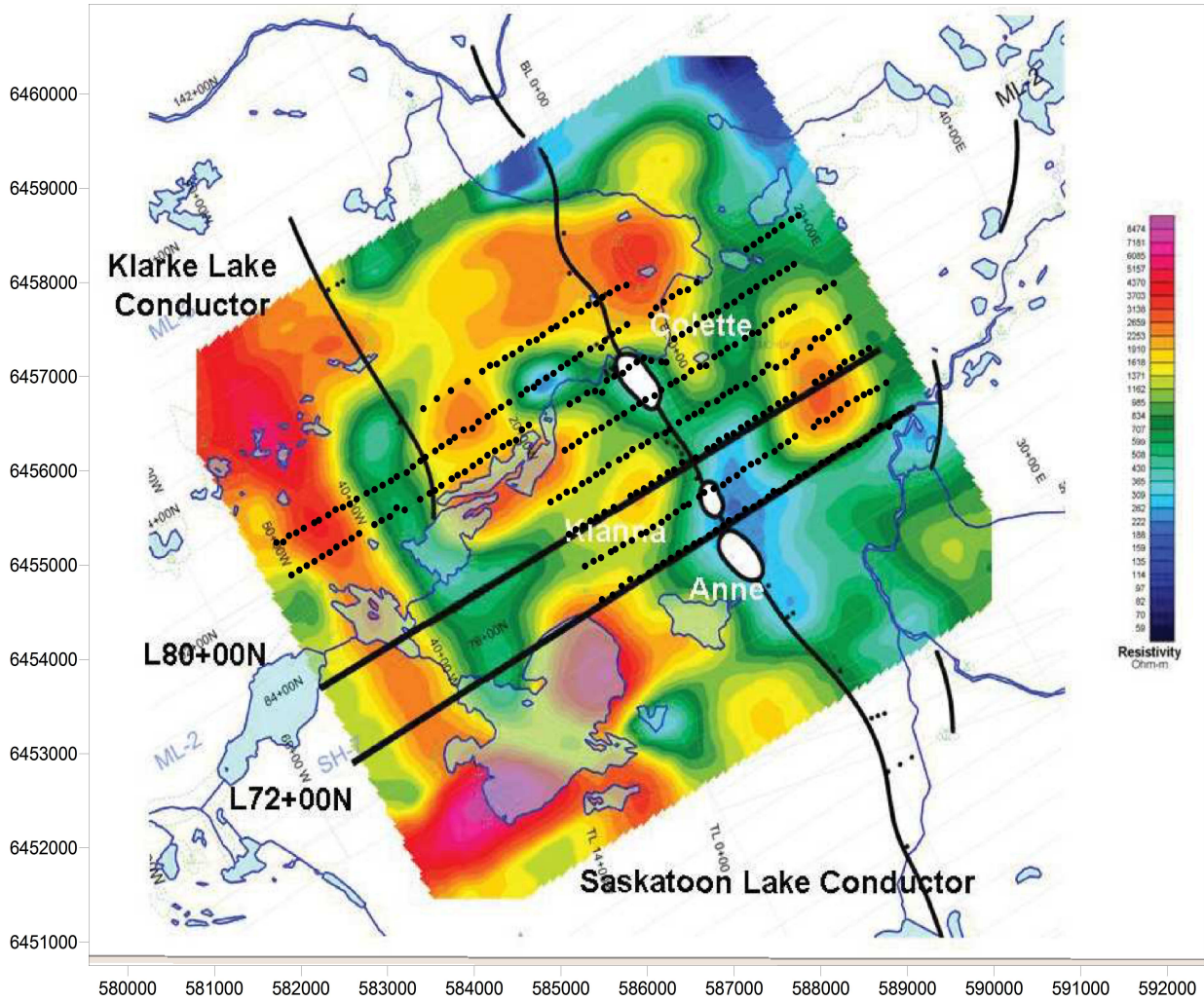


Figure 4: Horizontal slice out of 3D DC resistivity model at 600 m depth
Shea Creek 3D TAMT Inversion - 640 to 700 m Plz

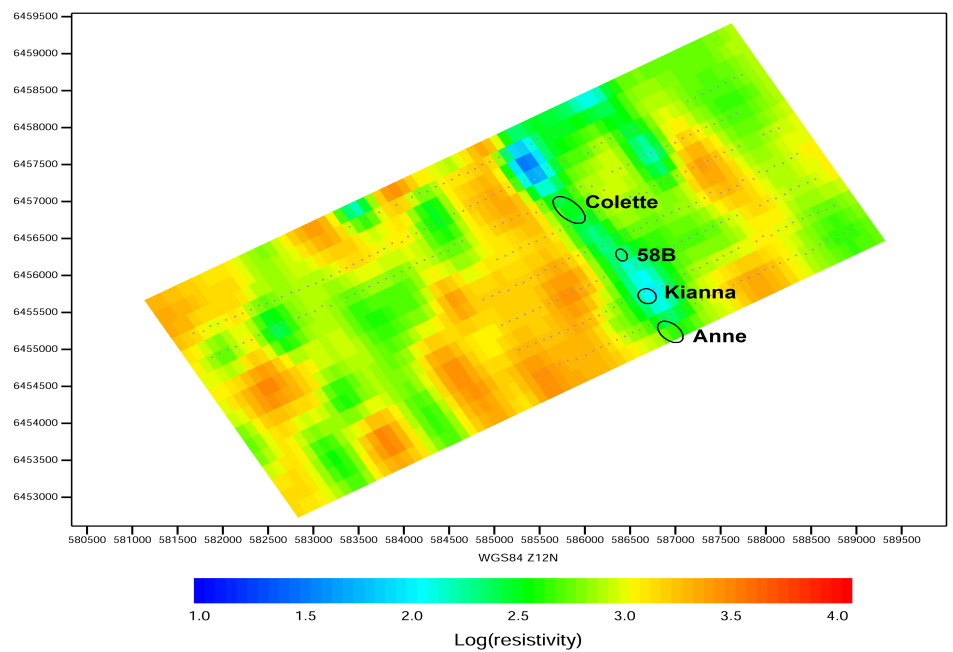


Figure 5: Horizontal slice out of tipper inverted 3D model

Shea Creek L80N 3D TAMT Inversion

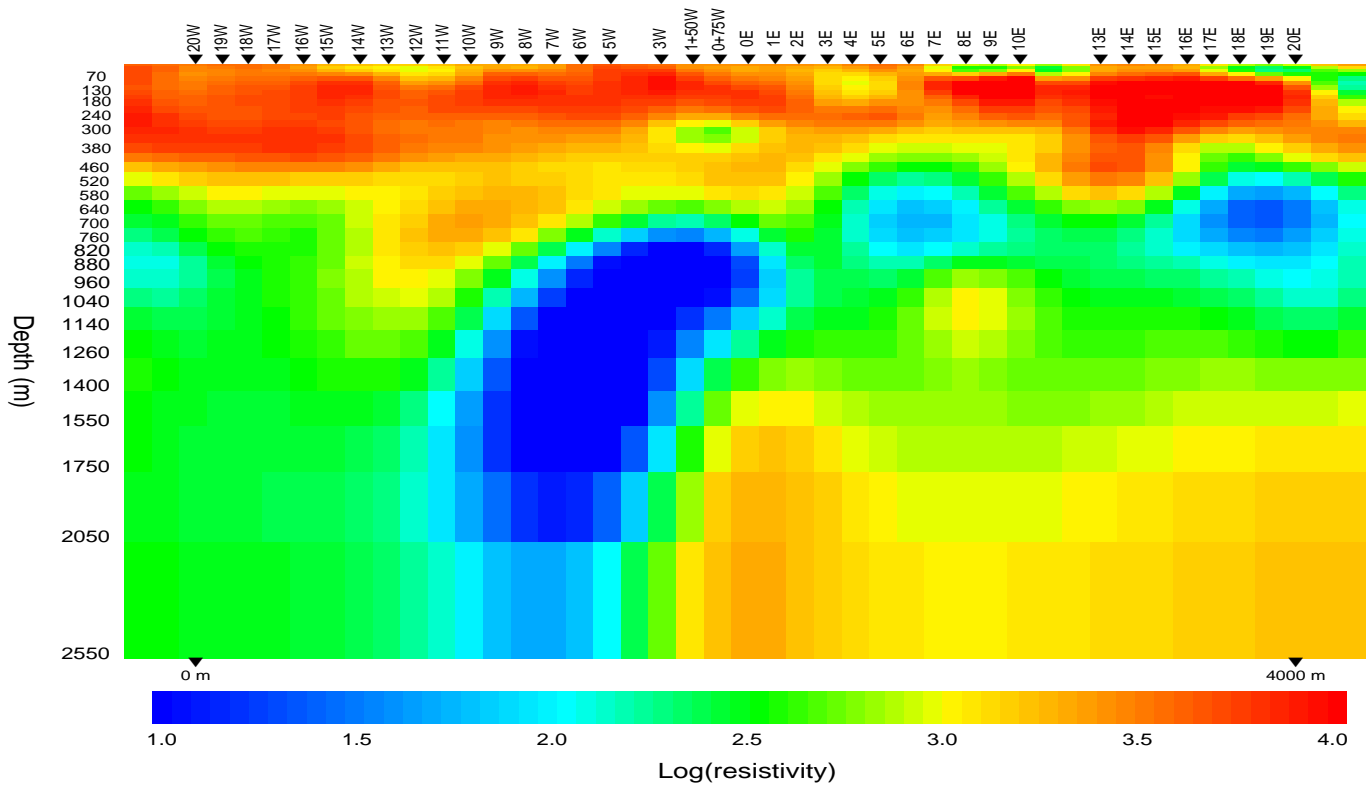


Figure 6: Vertical Slice out of joint impedance-tipper 3D model down L80N

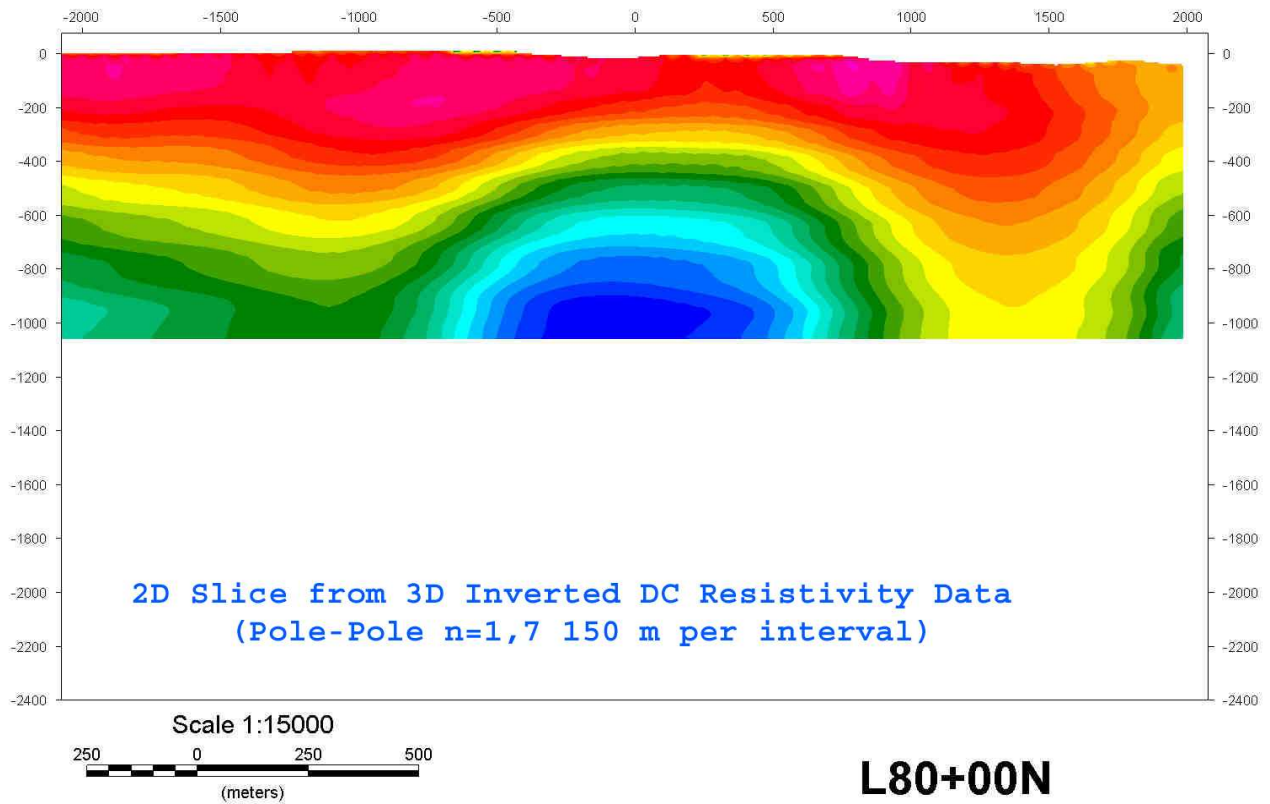


Figure 7: Vertical Slice out of tipper 3D model down L96N

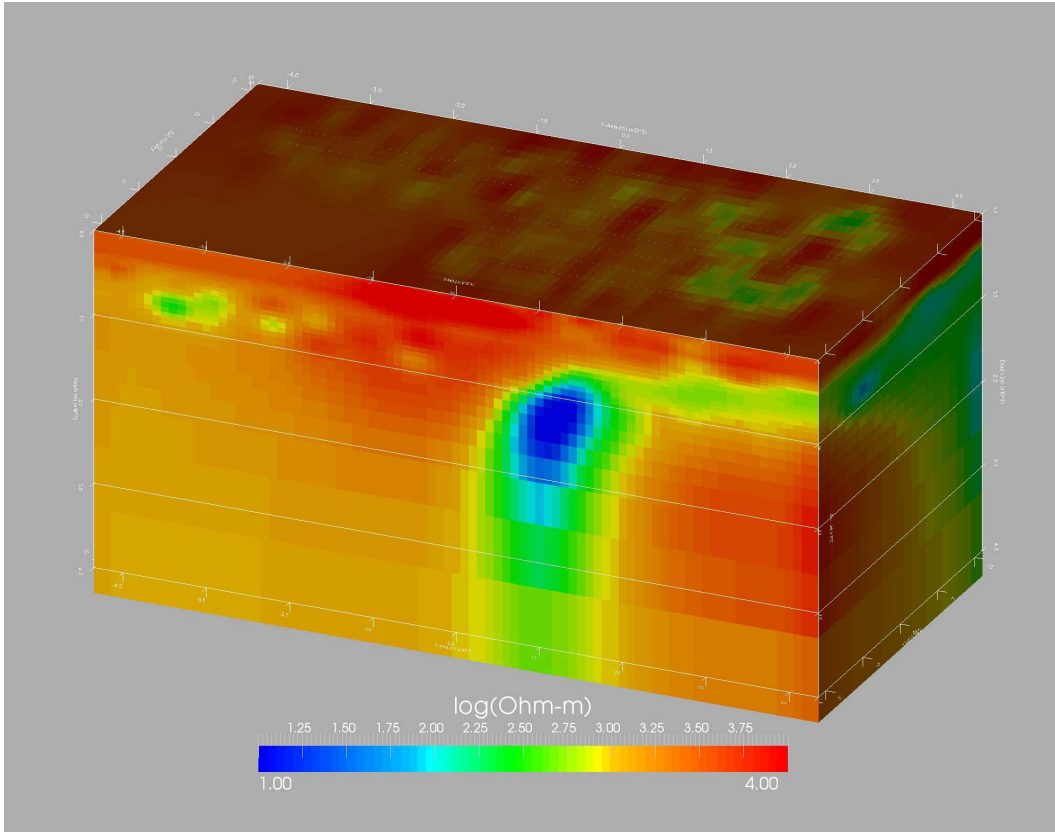


Figure 8: 3D Inversion Cube, looking North-West

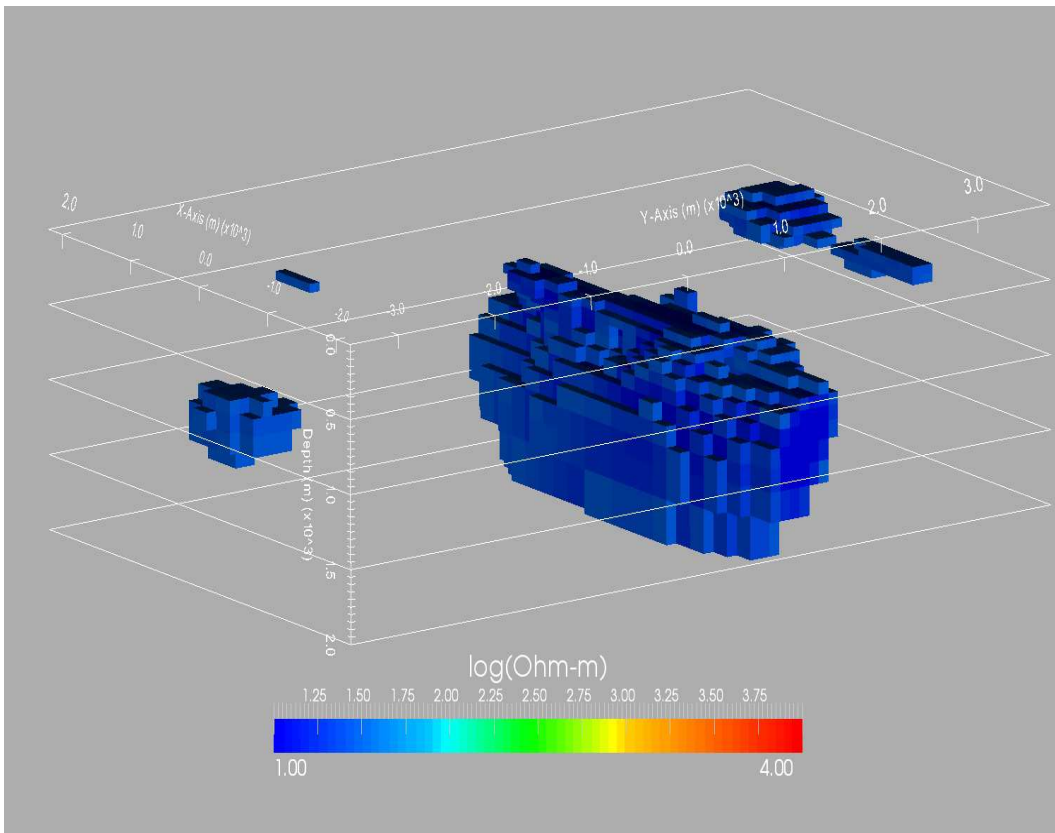


Figure 9: 3D Volumetric plot, looking North, $\leq 30 \Omega\text{-m}$

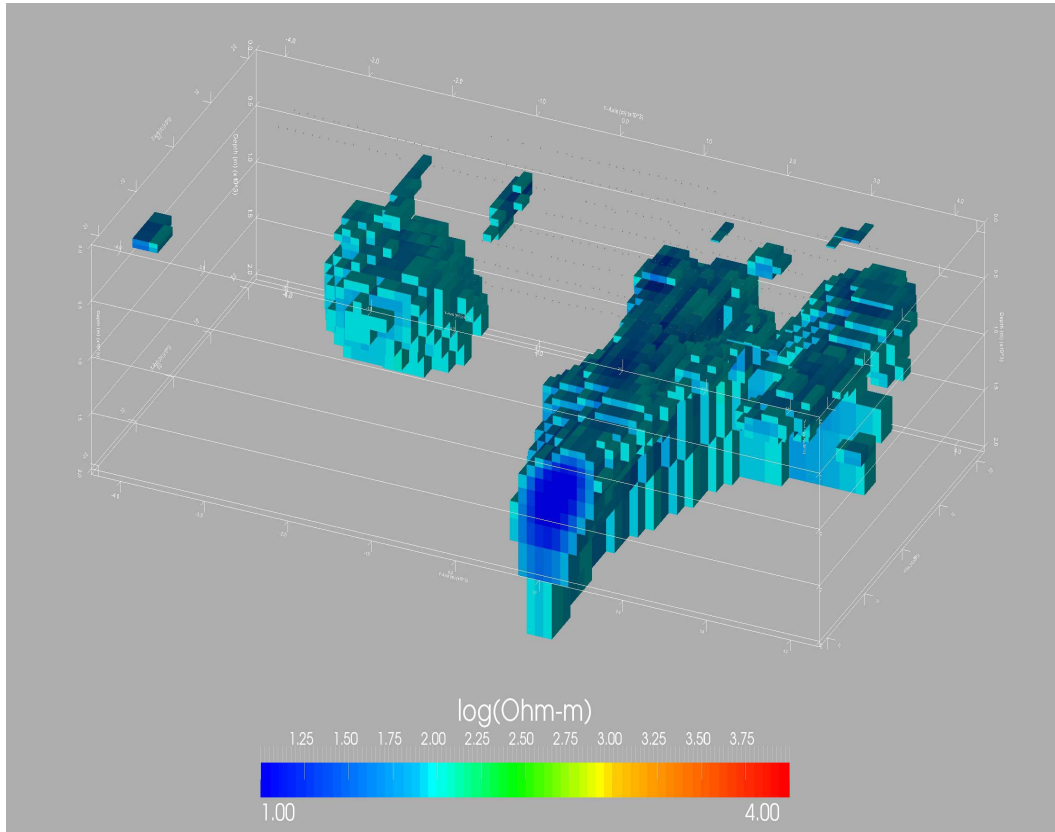


Figure 10: 3D Volumetric plot, looking North-West, $\leq 100 \Omega\text{-m}$

Shea Creek L72N 3D TAMT Inversion

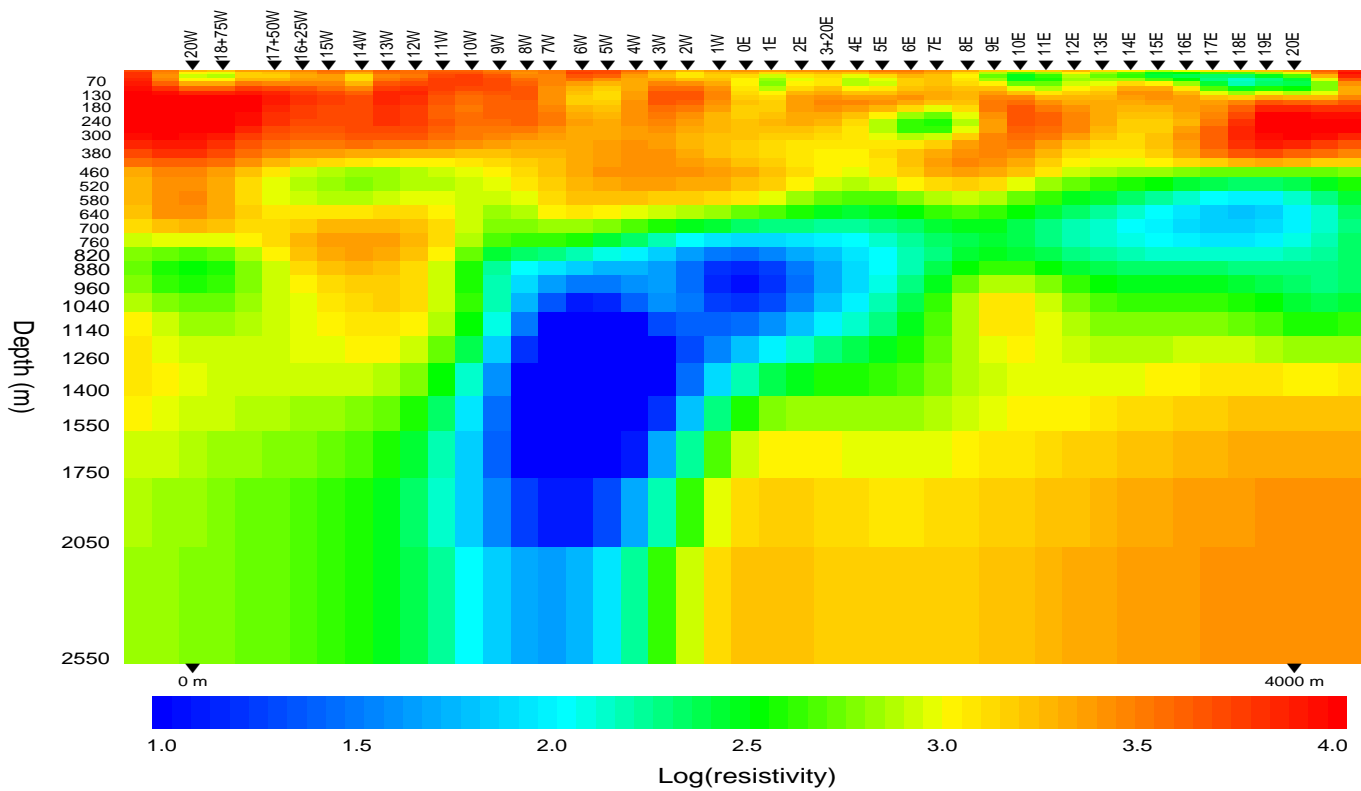


Figure 11: Vertical Slice out of joint impedance-tipper 3D model down L72N

Shea Creek L76N 3D TAMT Inversion

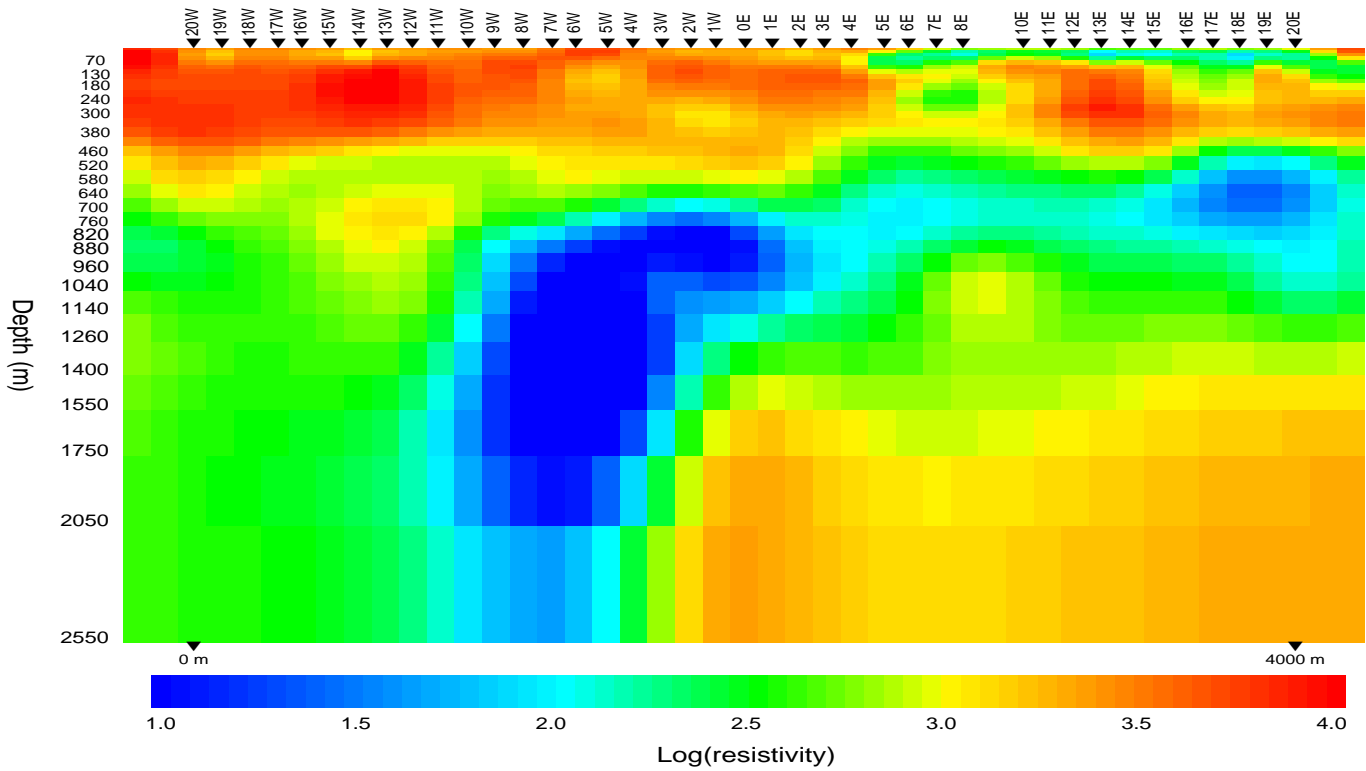


Figure 12: Vertical Slice out of joint impedance-tipper 3D model down L76N

Shea Creek L80N 3D TAMT Inversion

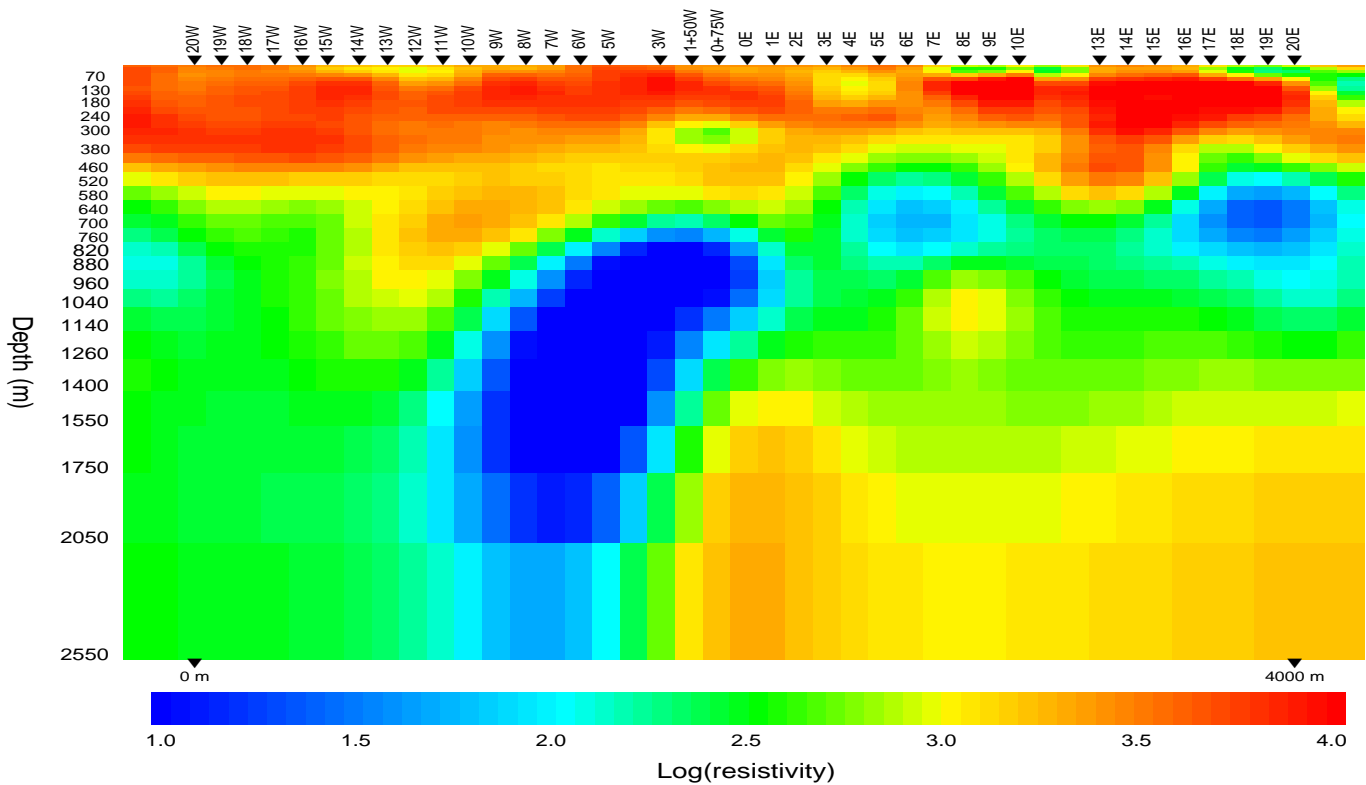


Figure 13: Vertical Slice out of joint impedance-tipper 3D model down L80N

Shea Creek L84N 3D TAMT Inversion

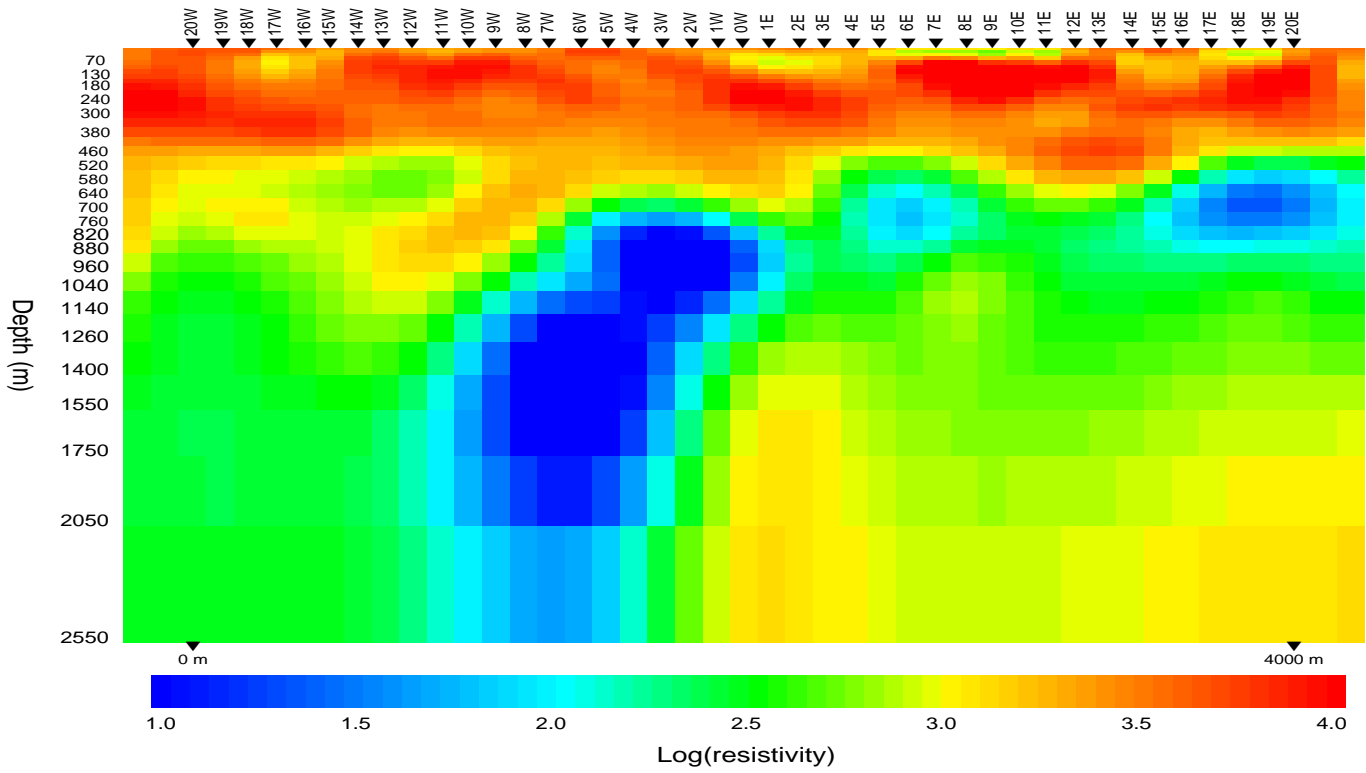


Figure 14: Vertical Slice out of joint impedance-tipper 3D model down L84N

Shea Creek L88N 3D TAMT Inversion

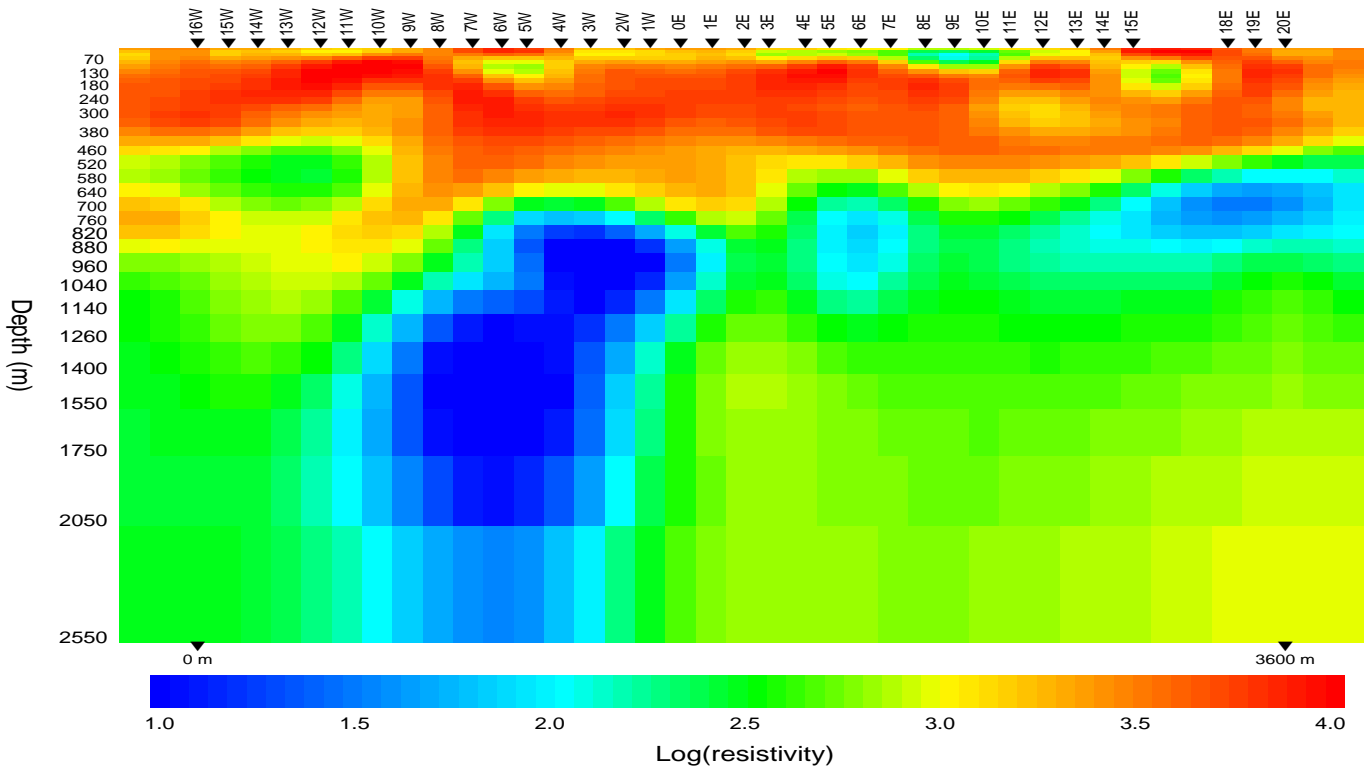


Figure 15: Vertical Slice out of joint impedance-tipper 3D model down L88N

Shea Creek L92N 3D TAMT Inversion

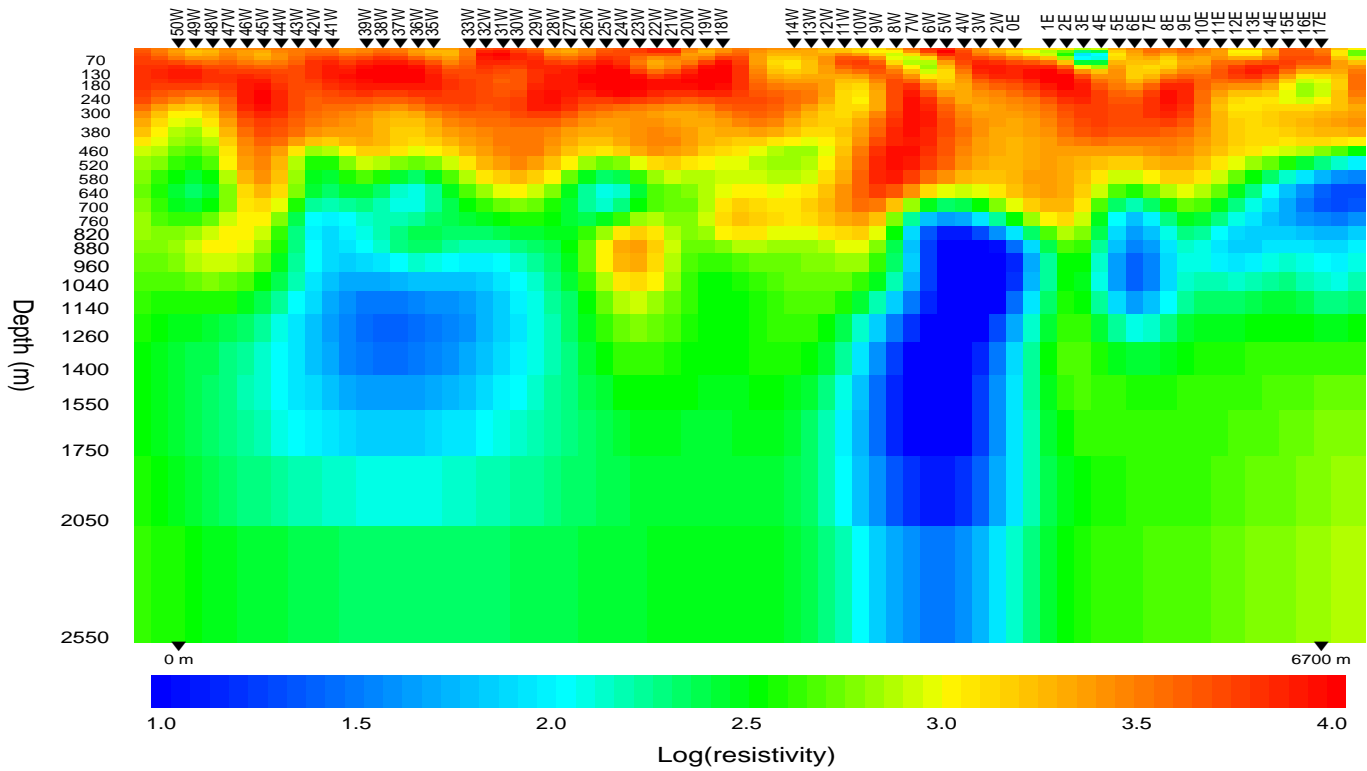


Figure 16: Vertical Slice out of joint impedance-tipper 3D model down L92N

Shea Creek L96N 3D TAMT Inversion

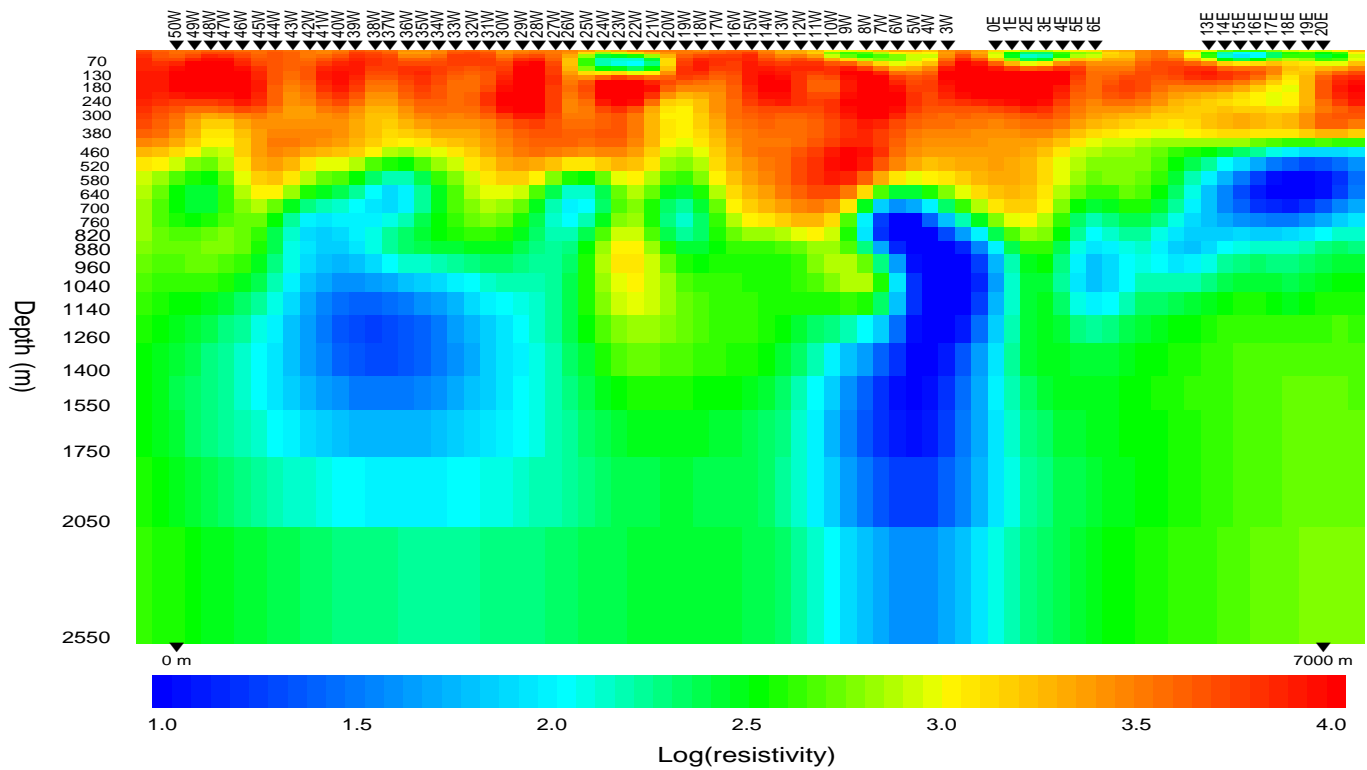


Figure 17: Vertical Slice out of joint impedance-tipper 3D model down L96N

Shea Creek L100N 3D TAMT Inversion

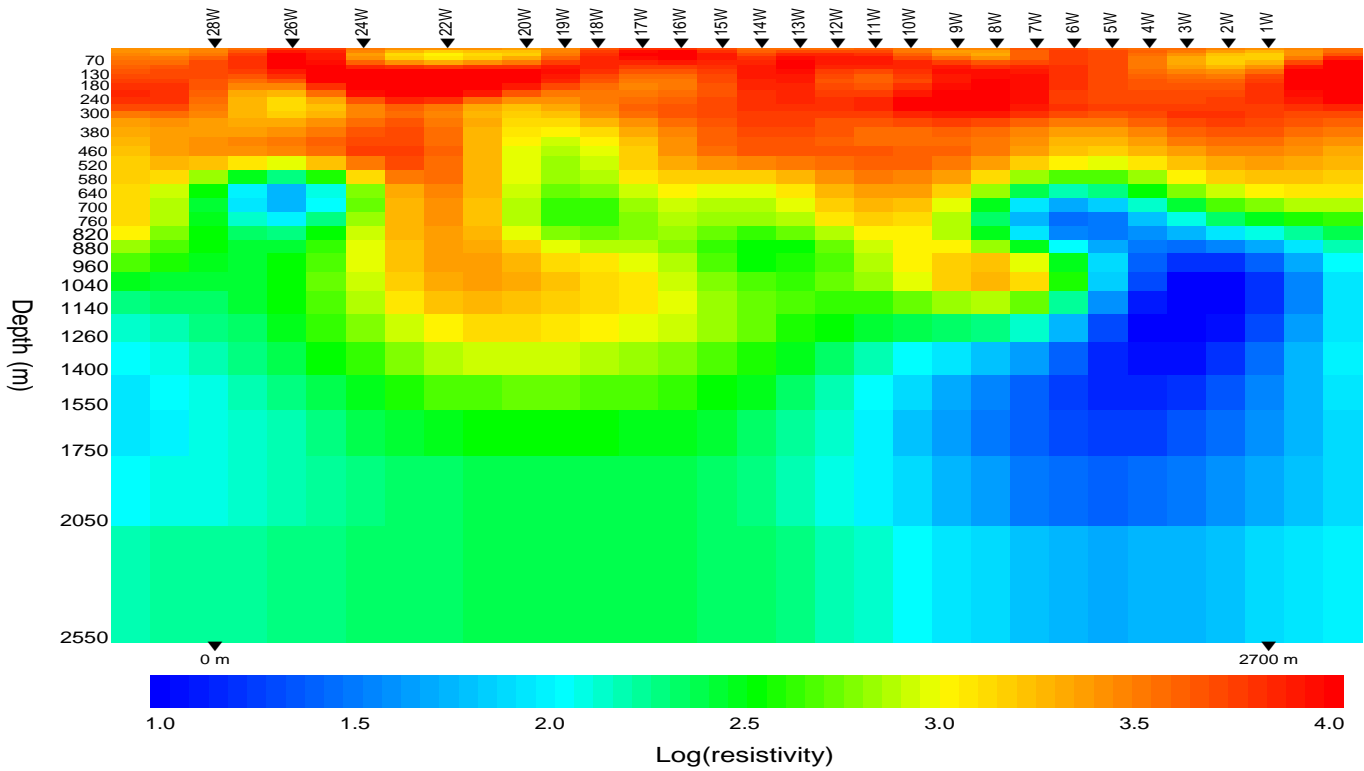


Figure 18: Vertical Slice out of joint impedance-tipper 3D model down L100N

Shea Creek L96N 3D TAMT Inversion

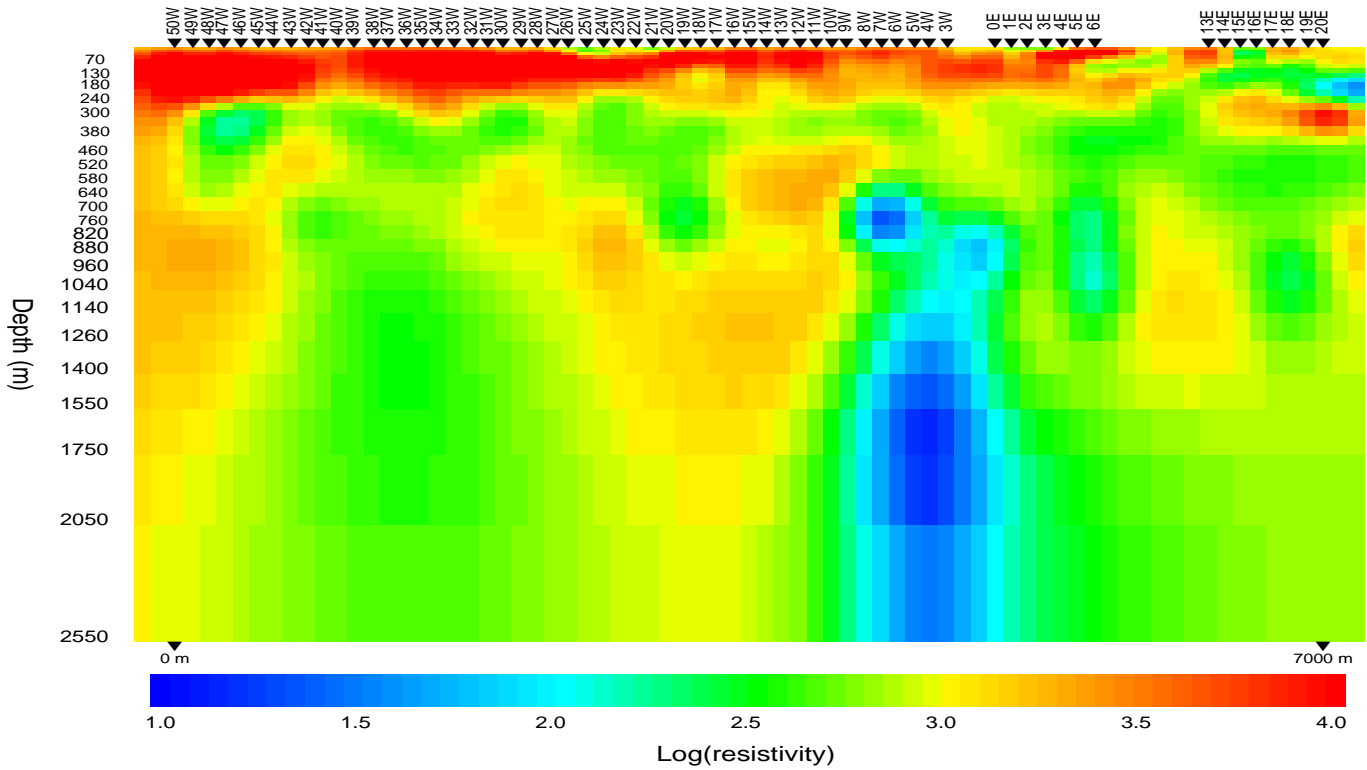


Figure 19: Vertical Slice out of tipper 3D model, down L96N